## Molecular dynamics simulations of the surface tension of n-hexane, n-decane and n-hexadecane

J. P. Nicolas; B. Smit

## PLEASE SCROLL DOWN FOR ARTICLE

# Molecular dynamics simulations of the surface tension of n-hexane, n-decane and n-hexadecane

J. P. NICOLAS and B. SMIT*

Department of Chemical Engineering, University of Amsterdam, Nieuwe
Achtergracht 166, 1018WV Amsterdam, The Netherlands

Molecular dynamics simulations have been used to compute the surface tension of linear alkanes. The OPLS force field has been compared with the SKS force field for alkanes (n-hexane, n-decane and n-hexadecane) over two ranges of temperature: high temperatures where no experimental data are available for surface tension and lower temperatures where comparisons may be made with experiments. At high temperatures, for a given coexistence density, these two models predict a similar surface tension. For a given temperature the two models yield different surface tensions. However, these deviations can be attributed to differences in the prediction of the coexistence curves. For the SKS model the computed coexistence properties have been compared with experimental data. The simulation data are in reasonable agreement with the experimental data.

## 1. Introduction

Alkanes are an important class of molecules that occur in many practical applications, and many molecular models have been developed to describe the interactions between alkanes [1–6]. In these studies the models have been tested via a comparison with the experimental vapour–liquid coexistence curve. Subsequently, these models have been further validated via a comparison of the simulated and experimental diffusion coefficients [7] and viscosities [8, 9]. Less attention has been given to the surface tension.

We have compared the predictions of two alkane models to obtain some insight into the dependence of the computed surface tension on the details of the intermolecular interactions. We have computed the surface tension for the linear alkanes (n-hexane, n-decane and n-hexadecane) using OPLS [10] and SKS force field models. We have performed the simulation over two temperature ranges. One temperature range is the same as in [11] in which Alejandre and coworkers computed the surface tension of hexane at coexistence (vapour–liquid) for high temperatures using the SKS and de Pablo [12, 13] models. Our results for the surface tension of the hydrocarbons can be compared with the simulation data of Alejandre and coworkers. This allows us to validate our program and extend their results to other chain lengths and temperaures. However, to the best of our knowledge, there are no experimental data

available for these systems at coexistence. Therefore, we do not know how accurately these alkane models can predict the surface tension. Experimental data are available at much lower temperatures, at densities higher than the coexistence density. We performed simulations under these conditions to assess the accuracy of the predicted surface tensions.

## 2. Models and simulation methodology
### 2.1. *Force fields*

We calculate the surface tension for liquid/gas systems of the linear alkanes hexane, decane, hexadecane. Two sets of force fields, SKS and OPLS, are compared.

We use the united atom representation, which means that every methylene ($CH_2$) or methyl ($CH_3$) group is modelled as a single interaction site. Three types of potential are employed: non-bonded interaction, bond bending and torsion potentials. The non-bonded interactions between united atoms from different molecules and within a molecule (if two atoms are more than four atoms apart) are described with a Lennard-Jones potential. The interactions are truncated and shifted with a cutoff radius $r_c$:

$$u(r_{ij}) = \begin{cases} u(r_{ij})^{LJ} - u(r_c)^{LJ} & r_{ij} < r_c, \\ 0 & r_{ij} > r_c, \end{cases} \quad (1)$$

with

$$u(r_{ij})^{LJ} = 4\varepsilon_{ij}\left[\left(\frac{\sigma_{ij}}{r_{ij}}\right)^{12} - \left(\frac{\sigma_{ij}}{r_{ij}}\right)^6\right], \quad (2)$$

* Author for correspondence. e-mail: b.smit@science.uva.nl

Table 1. Values of the Lennard-Jones parameters and $r_c$ from the SKS and OPLS models [1, 16].

|  | CH$_2$ | | CH$_3$ | | |
| --- | --- | --- | --- | --- | --- |
|  | $\sigma/\text{Å}$ | $\varepsilon/K$ | $\sigma/\text{Å}$ | $\varepsilon/K$ | $r_c/\text{Å}$ |
| SKS | 3.93 | 47.0 | 3.93 | 114 | 13.8 |
| OPLS | 3.905 | 59.4 | 3.905 | 88.1 | 11.5 |

where $r_{ij}$ is the distance between united atoms $i$ and $j$, $r_c$ is the cutoff distance, and $\varepsilon$ and $\sigma$ are Lennard-Jones energy and distance parameters, respectively. The numerical values of these parameters are shown in table 1. $\varepsilon_{ij}, \varepsilon_i, \varepsilon_j$ and $\sigma_{ij}, \sigma_i, \sigma_j$ are related by $\varepsilon_{ij} = (\varepsilon_i \varepsilon_j)^{1/2}$ and $\sigma_{ij} = (\sigma_i + \sigma_j)/2$, respectively.

We use a fixed bond length of 1.53 Å using the SHAKE algorithm [14]. The bond-bending potential is given by [15]:

$$u^{\text{bend}}(\theta) = \tfrac{1}{2}k_\theta(\theta - \theta_0)^2, \qquad (3)$$

where $\theta$ is the angle between two connected bonds, $\theta_0$ is the equilibrium value of this angle, and $k_\theta$ the force constant. We have used $k_\theta = 62\,500 \text{ K rad}^{-2}$ for both models, $\theta_0 = 112°$ in the OPLS model and $114°$ in the SKS model.

The torsion potential is defined for the OPLS model [16]:

$$u^{\text{tors}}_{\text{OPLS}}(\phi) = \sum_{k=0}^{5} c_k \cos^k(\phi), \qquad (4)$$

and for the SKS model:

$$u^{\text{tors}}_{\text{SKS}}(\phi) = 0.5[c_1(1 + \cos\phi) + c_2(1 - \cos 2\phi)$$
$$+ c_3(1 + \cos 3\phi)], \qquad (5)$$

where $\phi$ is the dihedral angle. In the OPLS model, we use $c_0 = 1116 \text{ K}$, $c_1 = 1462 \text{ K}$, $c_2 = -1578 \text{ K}$, $c_3 = -368 \text{ K}$, $c_4 = 3156 \text{ K}$, $c_5 = -3788 \text{ K}$. For the SKS model we use $c_1 = 355 \text{ K}$, $c_2 = -68.19 \text{ K}$ and $c_3 = 791.3 \text{ K}$.

### 2.2. Surface tension calculation

The surface tension $\gamma$ is proportional to the integral of the difference between the normal $P_N(z)$ and tangential $P_T(z)$ components of the pressure tensor. For an interface normal to the $z$ axis, the expression for the surface tension reads:

$$\gamma = \frac{1}{2} \int_{-L_z/2}^{+L_z/2} dz[P_N(z) - P_T(z)], \qquad (6)$$

where $L_z$ is the length of the simulation box along $z$ axis, perpendicular to liquid–gas interfaces, and 1/2 a corrector factor when the simulation box contains two interfaces.

The profile components of the pressure tensor are obtained using the Irving and Kirkwood definition [17, 18]:

$$P_T(z) = \langle \rho(z) \rangle k_B T - \frac{1}{A} \left\langle \sum_i \sum_{j>i} \frac{(x_{ij}^2 + y_{ij}^2)}{2r_{ij}} \right.$$
$$\left. \times \frac{dU_{\text{int}}(r_{ij})}{dr_{ij}} \frac{1}{|z_{ij}|} \theta\left(\frac{z - z_i}{z_{ij}}\right) \theta\left(\frac{z_{ij}}{z_j - z}\right) \right\rangle, \quad (7)$$

$$P_N(z) = \langle \rho(z) \rangle k_B T - \frac{1}{A} \left\langle \sum_i \sum_{j>i} \frac{z_{ij}^2}{2r_{ij}} \frac{dU_{\text{int}}(r_{ij})}{dr_{ij}} \right.$$
$$\left. \times \frac{1}{|z_{ij}|} \theta\left(\frac{z - z_i}{z_{ij}}\right) \theta\left(\frac{z_{ij}}{z_j - z}\right) \right\rangle, \qquad (8)$$

where $\rho(z)$ is the density profile along the $z$ direction, $k_B$ Boltzmann's constant, $T$ the temperature, $A = L_x \times L_y$ the area of one interface, $x_{ij}, y_{ij}, z_{ij}$ are the $x, y, z$ components of the distance $r_{ij}$ between united atoms $i$ and $j$, respectively, $\langle \cdots \rangle$ the canonical ensemble average, $U_{\text{int}}$ the potential energy, and $\theta(z)$ the Heaviside step function.

The components of the pressure tensor are computed by dividing the simulation box into $N_{\text{slabs}}$ slabs, parallel to the $xy$ interface, and the contribution of each interaction between united atoms $i$ and $j$ to the surface tension (including bond constraints from the SHAKE algorithm) is distributed in the slabs involved, i.e. slabs in which the particles $i$ and $j$ reside and slabs in between [19].

### 2.3. Simulations

Our simulations were performed in the $NVT$ ensemble [20], i.e. with constant temperature, volume and number of particles. The equations of motion were solved using the Verlet leapfrog integration algorithm [21]. Simulations were run with periodic boundary conditions. We used the DLPOLY program [22] for all our simulations.

At high temperatures, we investigated the system at vapour–liquid coexistence (with liquid and gas densities from Gibbs ensemble results) and at low temperatures the system was defined off-coexistence (with experimental liquid densities and vacuum). At coexistence we compared our simulation results with those from Alejandre et al. [11] and at lower temperatures with experimental data [23, 24].

The simulations at coexistence were initiated in the following way. First, we constructed a cubic box with molecules placed on a lattice at the estimated liquid density from Gibbs ensemble calculations [1]. For hexane, decane, and hexadecane the simulation cell contained 675, 405, and 300 molecules, respectively. This box was equilibrated for 50 000 timesteps with a time-

step $\Delta t = 3$ fs. Next, two cubic cells with the same $xy$ size were added in the $z$ direction. These boxes were filled with a few alkane molecules to obtain the vapour coexistence density.

At low temperatures, off coexistence, we initiated the simulation at the liquid density taken from experimental data. For this range of temperature, the vapour pressure is so low that the gas boxes contain on average less than one molecule. Therefore, we used for these simulations empty boxes, and ran a few hundred steps in order to stabilize the interface. After this equilibration, liquid and gas boxes were approximately the same volume and the box length in $z$ direction exceeded 100 Å.

We accumulated surface tension values every 500 steps during 3 ns. These data were analysed using the block average method [25].

## 3. Results and discussion
### 3.1. *Liquid densities*

Before discussing the results for the surface tension, we shall compare the simulated liquid densities for the various models with experimental data. An example of a computed density profile of hexane at coexistence using the SKS model is presented in figure 1. This plot shows liquid–vapour coexistence. Because of the periodic boundary conditions we obtain two interfaces. From this figure we can compute the coexistence densities of the liquid with reasonable accuracy. Good agreement is found between results from simulations and those from experiments [26]. For the gas density, however, the number of molecules is too small for the coexistence gas density to be determined accurately. Figure 2 presents the coexistence liquid densities for hexane at various temperatures as obtained from our simulations using the SKS model, and it shows that the Gibbs ensemble results [1] are in reasonable but not perfect agreement with the present simulations. Important to note is that the Gibbs ensemble simulations used a trun-

cated potential [1], while in this work a truncated and shifted potential is used. For a simple Lennard-Jones fluid a truncated but not shifted potential has a 10% higher critical temperature [27, 28]. A similar shift of the critical temperature has been observed here. In figure 2 we compare our results also with the MD simulations of Alejandre *et al.* [11], who used a similar method as in the present work to compute the coexistence properties. However, in the work of Alejandre *et al.* a slightly larger cutoff radius (15 Å) together with an inhomogeneous tail correction were used compared with Gibbs ensemble simulations [1, 29]. This results in a higher $T_c$ and hence a higher coexistence density compared with our simulations. For hexane also the OPLS model gives a good description of the experimental data.

Figure 2. Comparison of the liquid coexistence densities, for n-hexane (top), n-decane (centre) and n-hexadecane (bottom) at coexistence, as a function of temperature, for the present work, the Gibbs ensemble results [2], the results from Alejandre *et al.* molecular dynamic simulations [11] and experimental results concerning hexane [26].
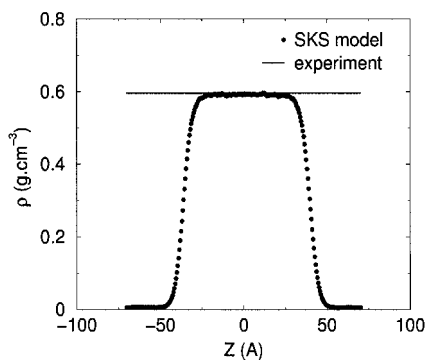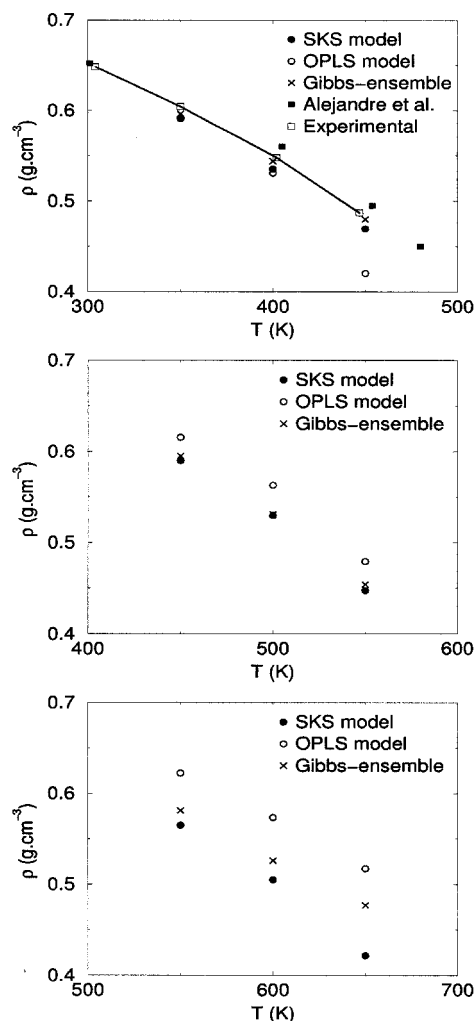
Figure 1. Density profile of hexane at coexistence at 350 K as obtained from the molecular dynamic simulations using the SKS model. The solid line gives the experimental value of liquid density [26] at this temperature.
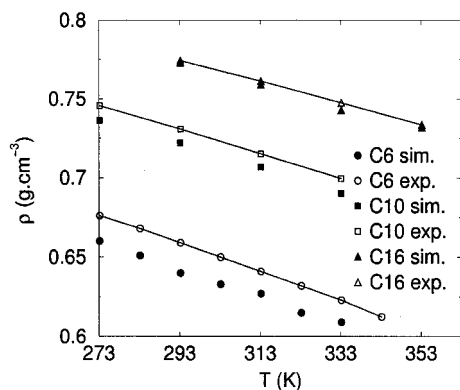
Figure 3.    Density $\rho$ for the SKS model and experiments.

Concerning the highest temperature, the interfaces are not well defined, and thus do not yield an accurate estimation of the liquid density.

For n-decane and n-hexadecane, figure 2 shows that the SKS model predicts a lower liquid density, compared with the OPLS model, which is consistent with the conclusion in [1] that the OPLS model overestimates the critical temperatures for the long chain alkanes.

Figure 3 compares the simulated liquid densities at low temperature (off-coexistence), using the SKS model, with the experimental liquid densities where the surface tension has been determined experimentally. For n-decane and n-hexadecane the agreement with the experimental data is very good, while for n-hexane, the simulations underestimate the liquid densities.

### 3.2. *Surface tension estimations*

In figure 4, the calculated surface tension for hexane, decane, and hexadecane at coexistence are shown as a function of the temperature and density. To the best of our knowledge, experimental data for these systems have not been published. For hexane we can compare the surface tension as a function of the temperature as obtained by our simulations with the results obtained by Alejandre *et al.* [11]. The agreement between these two studies is satisfactory; the small differences can be related to the larger cutoff radius used by Alejandre *et al.* For the OPLS model a similar result is obtained. If we plot the results versus liquid densities the differences between the various models become much smaller.

For n-decane and n-hexadecane the differences between simulated surface tension as a function of the temperature of the OPLS and SKS model are larger compared with hexane. Also, for these molecules the differences disappear if we plot the surface tension as a function of the densities. Important to note is that for a given coexistence density the computed surface tensions of the OPLS and SKS model are obtained at different temperatures. This suggests that the density is an im-
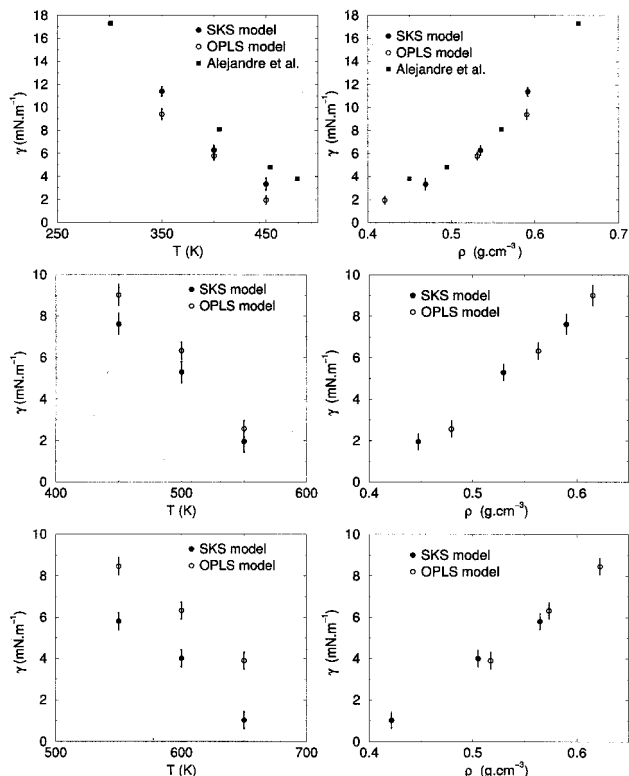


Figure 4.    Surface tension $\gamma$ versus $T$ (left) and $\rho$ (right) for $C_6$ (top), $C_{10}$ (centre) and $C_{16}$ (bottom), at coexistence.
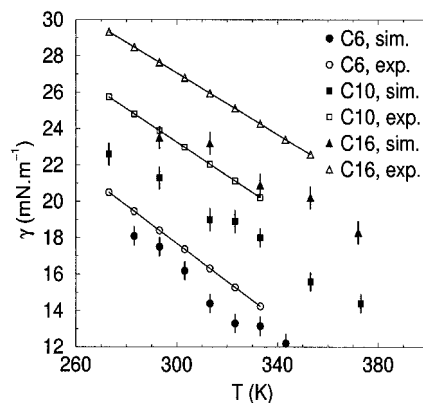


Figure 5.    Surface tension $\gamma$ versus $T$ as obtained from the simulations using the SKS model (solid symbols) compared with experimental data (lines and open symbols) [23, 24].

portant parameter when determining the surface tension.

Since the SKS model gives a better prediction of general properties at coexistence for the long chain alkanes [1, 30], we use this model for the simulation water conditions where the surface tension has been measured. Figure 3 showed that the simulations overestimate the liquid densities at these conditions. Figure 5 shows that, plotted versus $T$, the surface tension of the alkanes is

underestimated by about 15% compared with experimental results, independently of the temperature and the length of alkanes considered.

## 4. Conclusion

In this work we have computed liquid densities and the surface tension of various linear alkanes at various temperatures. For longer alkanes, the computed liquid densities confirm that they are better described by the SKS model than the OPLS model at high temperatures. At lower temperatures, the agreement between experimental and computed densities from the SKS model increases with the length of the linear alkanes.

The density prediction is a major parameter in surface tension calculations. Differences observed between the SKS and OPLS models in critical temperatures and liquid density predictions are cancelled when the predicted surface tension values are plotted as a function of the liquid density. At low temperatures, a comparison with experimental data shows that the surface tension is underestimated by approximately 15%.

Our simulations show that to predict the surface tension at a given temperature correctly, it is very important to use a model that predicts the density of the liquid phase at the given conditions sufficiently accurately. For example, the SKS model and the OPLS model give very similar results for the surface tension as a function of the liquid density. Therefore, if a given model does not predict the liquid density correctly such a model is of very limited value for predicting the surface tension.

## References

[1] SMIT, B., KARABORNI, S., and SIEPMANN, J. I., 1995, *J. chem. Phys.*, **102,** 2126.
[2] MONDELLO, M., and GREST, G. S., 1995, *J. chem. Phys.*, **103,** 7156.
[3] MARTIN, M. G., and SIEPMANN, J. I., 1997, *J. Amer. chem. Soc.*, **119,** 8921.
[4] NATH, S. K., ESCOBEDO, F. A., and DE PABLO, J. J., 1998, *J. chem. Phys.*, **108,** 9905.
[5] POTOFF, J. J., ERRINGTON, J. R., and PANAGIOTOPOULOS, A. Z., 1999, *Molec. Phys.*, **97,** 1073.
[6] DELHOMMELLE, J., BOUTIN, A., and FUCHS, A. H., 1999, *Molec. Simulation*, **22,** 351.
[7] MOORE, J. D., COCHRAN, H. D., and CUMMINGS, P. T., 2001, *J. chem. Phys.*, **113,** 8833.
[8] MCCABE, C., CUI, S., CUMMINGS, P. T., GORDON, P. A., and SAEGER, R. B., 2001, *J. chem. Phys.*, **114,** 1887.
[9] MONDELLO, M., GREST, G. S., WEBB III, E. B., and PECZAK, P., 1998, *J. chem. Phys.*, **109,** 798.
[10] JORGENSEN, W.L., MADURA, J. D., and SWENSON, C. J., 1984, *J. Amer. chem. Soc.*, **106,** 6638.
[11] ALEJANDRE, J. ,TILDESLEY, D. J., and CHAPELA, G. A., 1995, *Molec. Phys.*, **85,** 651.
[12] LASO, M., DE PABLO, J. J., and SUTER, U. W., 1992, *J. chem. Phys.*, **97,** 2817.
[13] DE PABLO, J. J., LASO, M., SIEPMANN, J. I., and SUTER, U. W., 1993, *Molec. Phys.*, **80,** 55.
[14] RYCKAERT, J.-P., CICCOTTI, G., and BERENDSEN, H. J. C., 1997, *J. comput. Phys.*, **23,** 327.
[15] VAN DER PLOEG, P., and BERENDSEN, H. J. C., 1982, *J. chem. Phys.*, **76,** 3271.
[16] RYCKAERT, J.-P., and BELLEMANS, A., 1975, *Chem. Phys. Lett.*, **30,** 123.
[17] WALTON, J. P. R. B., TILDESLEY, D. J., ROWLINSON, J. S., and HENDERSON, J. R., 1983, *Molec. Phys.*, **48,** 1357.
[18] KIRKWOOD, J. G., and BUFF, F. P., 1949, *J. chem. Phys.*, **17,** 338.
[19] NIJMEIJER, M. J. P., BAKKER, A. F., BRUIN, C., and SIKKENK, J. H., 1988, *J. chem. Phys.*, **89,** 3789.
[20] EVANS, D. J., and MORRISS, G. P., 1984, *Comput. Phys. Rep.*, **1,** 297.
[21] ALLEN, M. P., and TILDESLEY, D. J., 1989, *Computer Simulation of Liquids* (Oxford: Clarendon Press).
[22] DLPOLY 2.11 (Warrington, UK: Daresbury Laboratory, 1999).
[23] JASPER, J. J., KERR, E. R., and GREGORICH, F., 1953, *J. Amer. chem. Soc.*, **75,** 5252.
[24] JASPER, J. J., and KRING, E. V., 1955, *J. phys. Chem.*, **59,** 1019.
[25] FINCHAM, D., QUIRKE, N., and TILDESLEY, D. J., 1986, *J. chem. Phys.*, **84,** 4535.
[26] SMITH, B. D., and SRIVASTAVA, R., 1986, *Thermodynamics Data for Pure Compounds*, Part A, *Hydrocarbons and Ketones* (Amsterdam: Elsevier).
[27] SMIT, B., and FRENKEL, D., 1991, *J. chem. Phys.*, **94,** 5663.
[28] SMIT, B., 1992, *J. chem. Phys.*, **96,** 8639.
[29] SMIT, B., KARABORNI, S., and SIEPMANN, J. I., 1998, *J. chem. Phys.*, **109,** 352.
[30] MARTIN, M. G., and SIEPMANN, J. I., 1998, *J. phys. Chem. B*, **102,** 2569.